

# Towards observational fingerprints of African rainfall changes

Anna Lea Albright<sup>1</sup>, Michael Brenner<sup>2</sup>, Alessandra Giannini<sup>3</sup>, Peter Huybers<sup>1,2</sup>

<sup>1</sup>Harvard University, Department of Earth and Planetary Sciences, <sup>2</sup>Harvard Paulson School of Engineering and Applied Sciences, <sup>3</sup>École normale supérieure, Columbia University International Research Institute for Climate and Society

## Context and Data

- Drought in semiarid Sahel between ~1970-90 was one of the clearest regional climate signals and largest humanitarian disasters of 20th century (e.g., Nicholson 1980, Nicholson et al. 2000, Haywood et al., 2013, Nicholson et al., 2018); thought to result, in part, from cooling of North Atlantic by European and North American aerosols (e.g., Giannini et al., 2003, Held et al., 2005, Biasutti et al., 2008, Booth et al., 2012, Hwang et al., 2013, Giannini, Kaplan, 2019, Zhang et al., 2021)
- No agreement on whether the Sahel will be drier or wetter in the future (e.g., Held et al. 2005, Biasutti and Giannini 2006, Hoerling et al. 2006, Cook and Vizy 2006, Lickley et al., 2024)
- Regional climate predictions are generally more uncertain than global estimates, especially for rainfall, compared to other variables, and in Africa, compared to other regions. Here the goal is to:
  - identify coherent modes of historical rainfall variability in Africa,
  - deconvolve competing external forcings of these rainfall changes, and
  - provide observational benchmarks for climate models

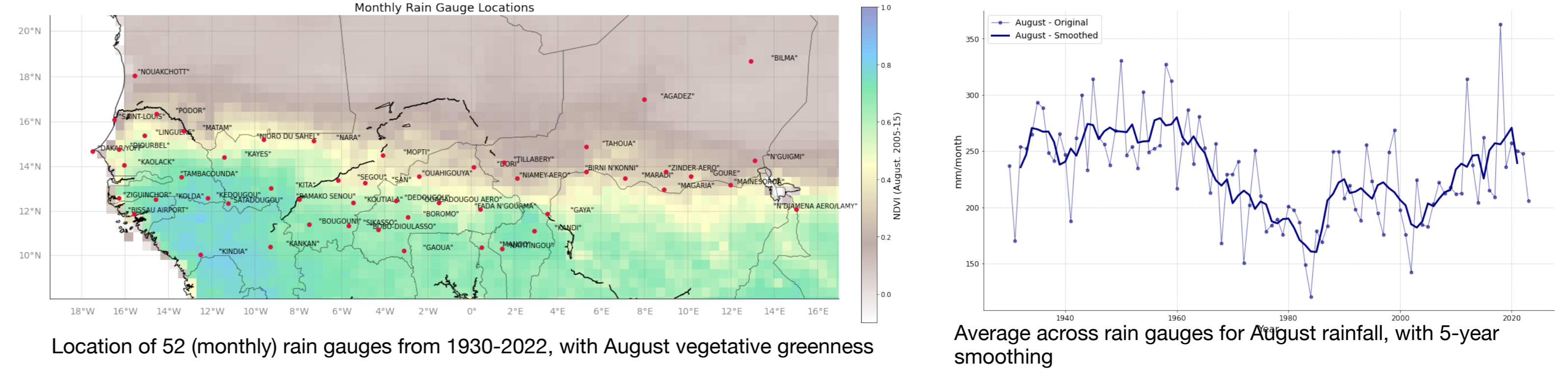
### Data

- Rain:**
  - IMERG: Integrated Multi-satellite Retrievals for GPM, 2001-22, satellite passive microwave sensors, Huffman et al., 2015
  - REGEN: rain gauges, gridded, 1950-2016, Contractor et al., 2020
  - Raw monthly (and daily) rain gauges
  - TAMSAT (Africa only): Tropical Applications of Meteorology using SATellite data and ground-based observations, 1983-2022, relates cloud top brightness temperature to rain rates, with rain gauges for calibration, Maidment et al., 2017
  - PERSIANN: Precipitation Estimation from Remote Sensed Information Using Artificial Neural Networks, 1983-2020, GridSat-B1 infrared satellite data, Ashouri et al., 2015
  - Accessed using FROGS data set, Roca et al., 2019
- NDVI for vegetative greenness**
- SSTs from HadISST**
- Land temperatures** from Berkeley Earth
- Multivariate ENSO index (MEI)**, Wolter, Timlin, 2011
- Climate models**
  - 1pctCO<sub>2</sub>-rad simulations, 1%/year increasing CO<sub>2</sub> coupled to the radiation code with control CO<sub>2</sub> concentrations applied to carbon cycle, in Coupled Climate Carbon Cycle Model Intercomparison Project (C4MIP), Jones et al., 2018
  - hist-aer, aerosol-only simulations, Detection and Attribution Model Intercomparison Projection (DAMIP), Gillett et al., 2016

## Coherent modes of rainfall variability

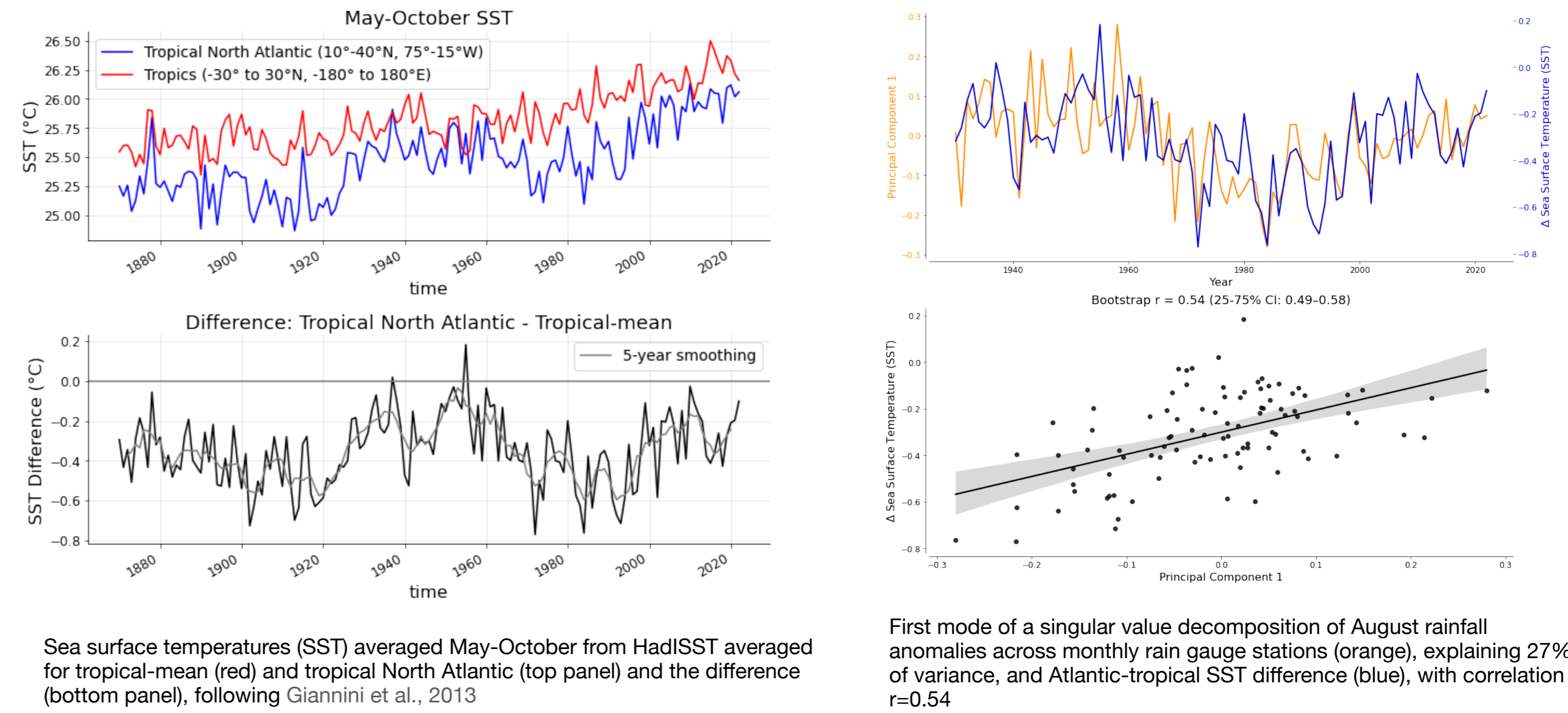
### Strong drying signal across Sahel rain gauges, peaking 1984

One of the clearest regional climate signals over 20th century, how well are physical mechanisms understood?



### Relative SSTs (tropical-mean - Atlantic SSTs) explain ~30% of variability in first mode of Sahelian summer rainfall (July-Sept.), following Giannini et al., 2013, cf. Vecchi et al., 2008

Tropical-mean temperatures set threshold for convection (e.g., Chiang and Sobel, 2002) and whether upped ante (Neelin et al., 2003) is reached depends on Atlantic SSTs and moisture/MSE advection in monsoon flow



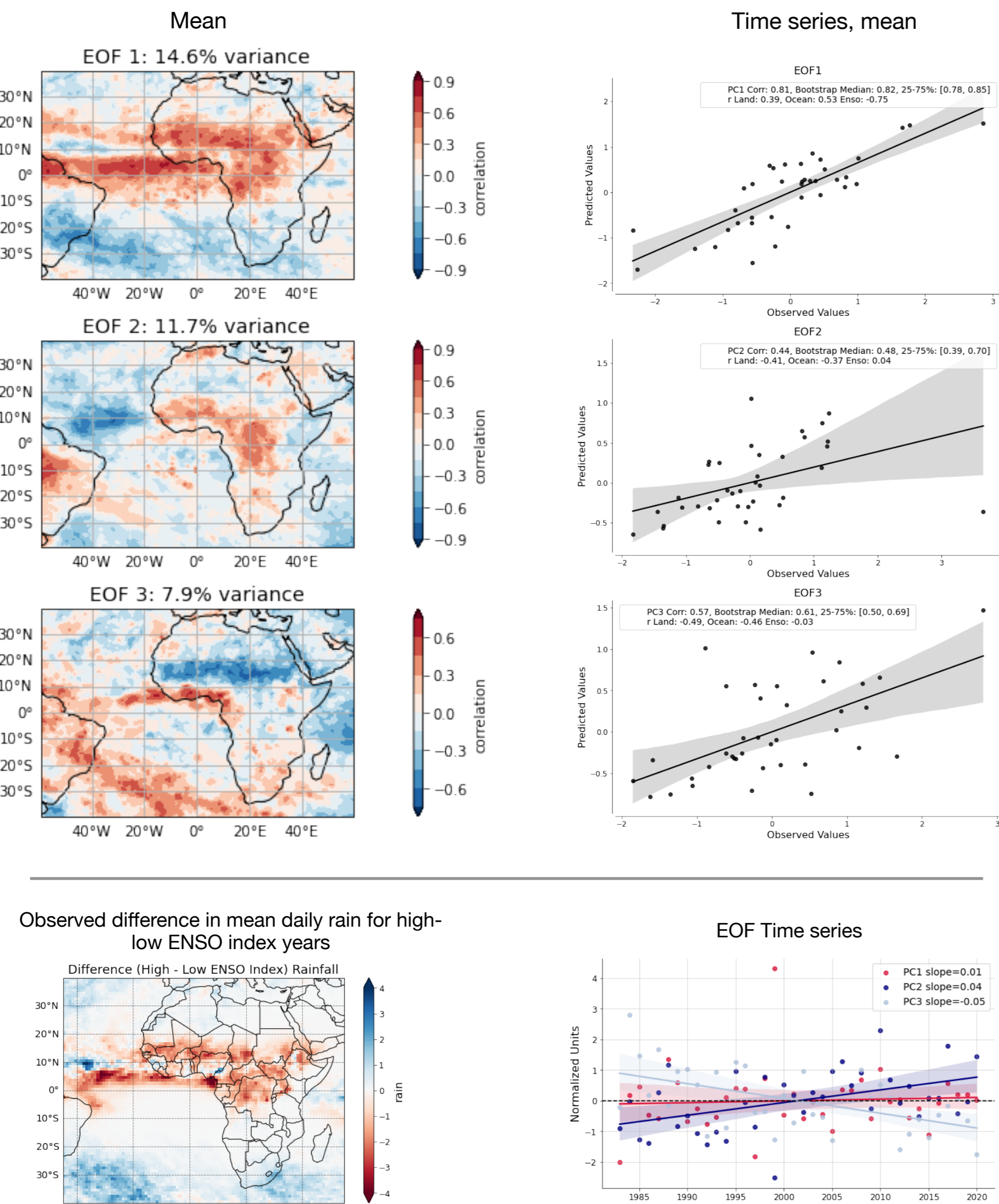
Sea surface temperatures (SST) averaged May-October from HadISST averaged for tropical-mean (red) and tropical North Atlantic (top panel) and the difference (bottom panel), following Giannini et al., 2013

First mode of a singular value decomposition of August rainfall anomalies across monthly rain gauge stations (orange), explaining 27% of variance, and Atlantic-tropical SST difference (blue), with correlation r=0.54

## Coherent modes of rainfall variability (II)

### Modes of June-Sept. rainfall variability

can, in part, be explained by ENSO, relative SST differences, Saharan temperature variability



Left column: three leading patterns of an empirical orthogonal function (EOF) analysis performed on June-September mean daily rainfall over Africa during 1983-2020 using the PERSIANN data set, with variance explained. Spatial patterns expressed as correlation of the time series and precipitation anomalies

Right column: time series of three leading EOFs and multiple linear regression of three variables considered, with individual correlations also listed:
 

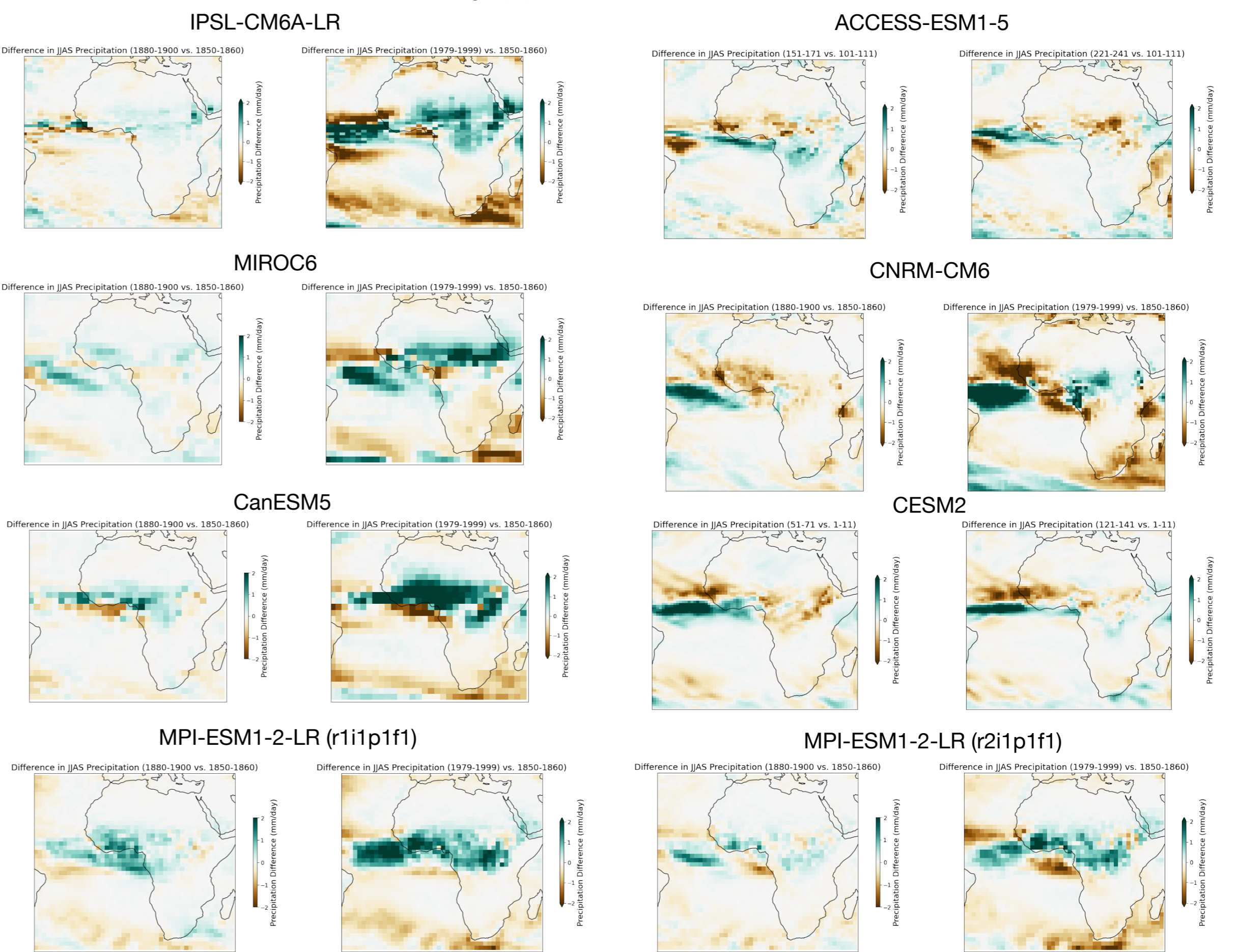
- MEI v2 ENSO index
- Atlantic minus tropical-mean SSTs following Giannini et al., 2013
- Saharan land temperatures (averaged 20-30 N, 20 W-20 E for June-Sept.)

First mode seems better explained by ENSO, second and third appear a combination of Saharan land temperatures & ocean relative SST differences

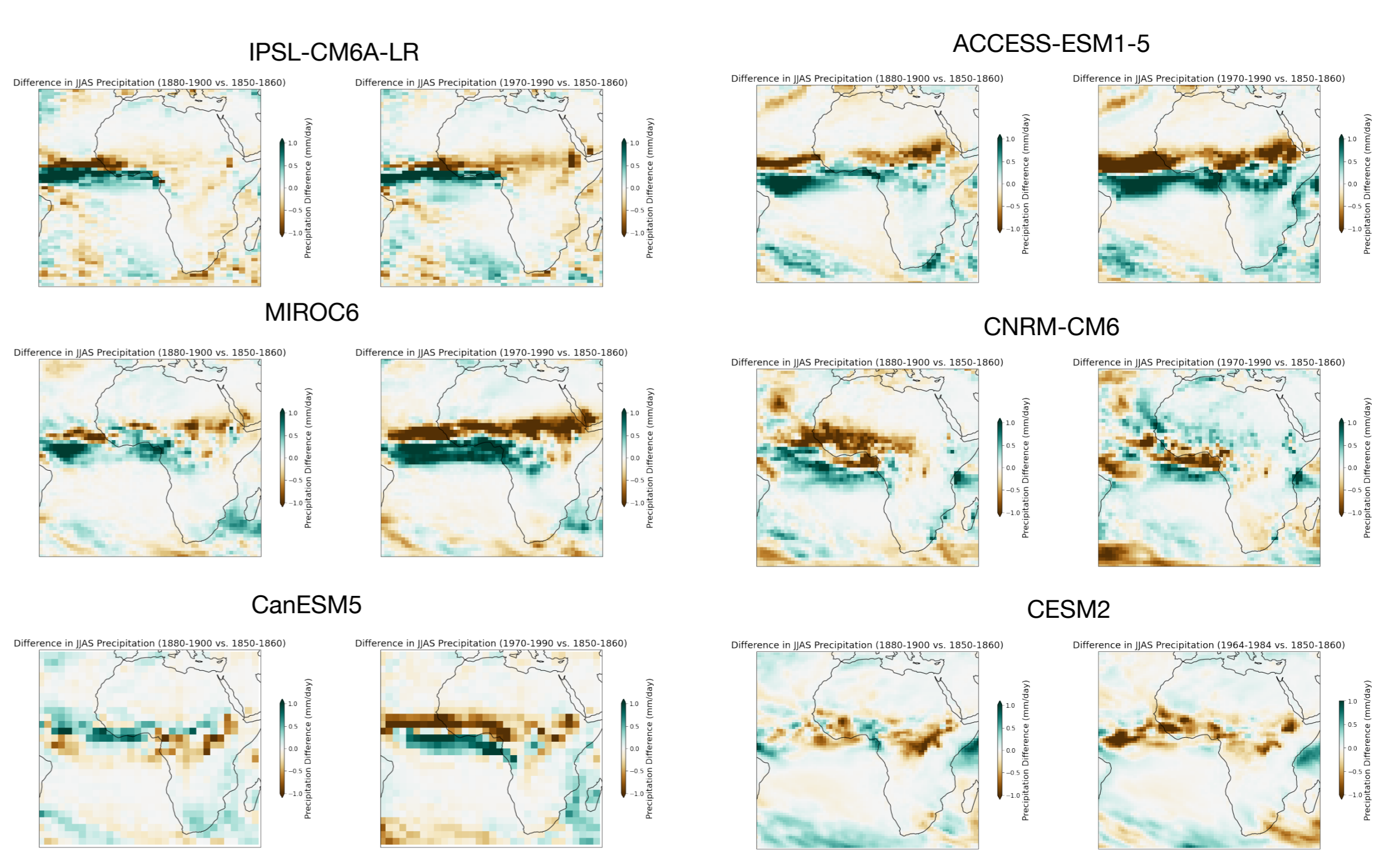
- Examine potential drivers in single-forcing simulations:
  - CO<sub>2</sub>
  - Aerosols
  - Sea surface temperatures

## Deconvolving physical drivers?

### CO<sub>2</sub> only (1pctCO<sub>2</sub>-rad) simulation



### Aerosol-only historical simulation (aer-hist)

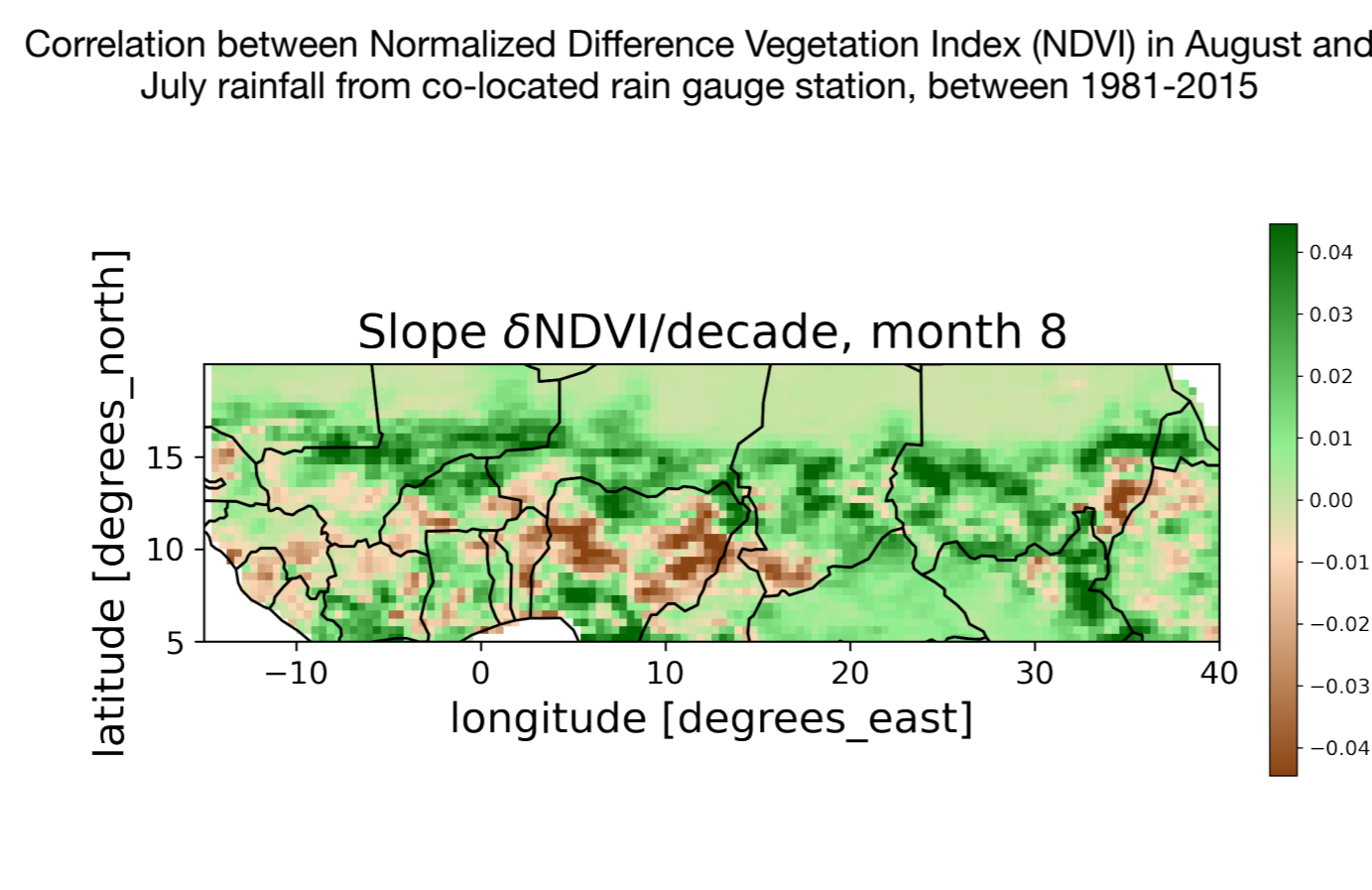
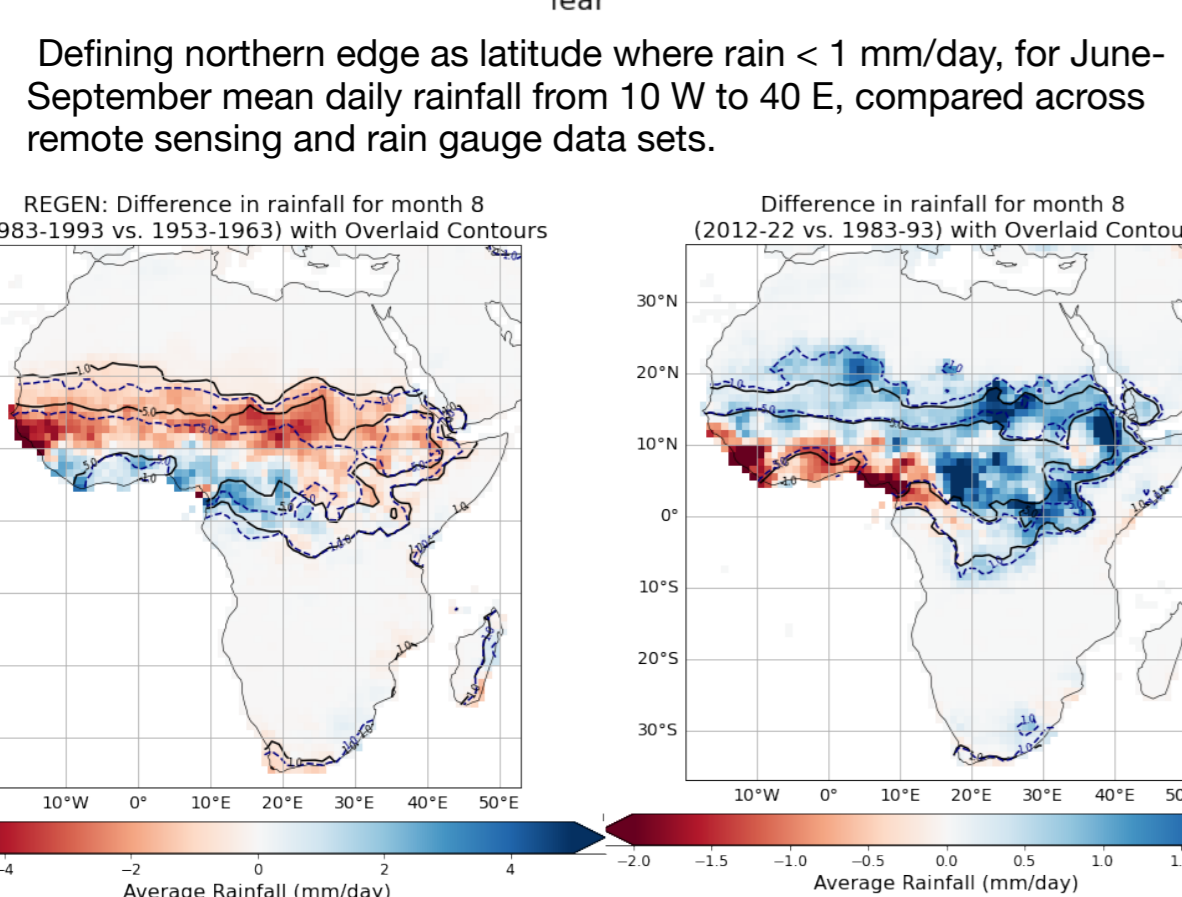
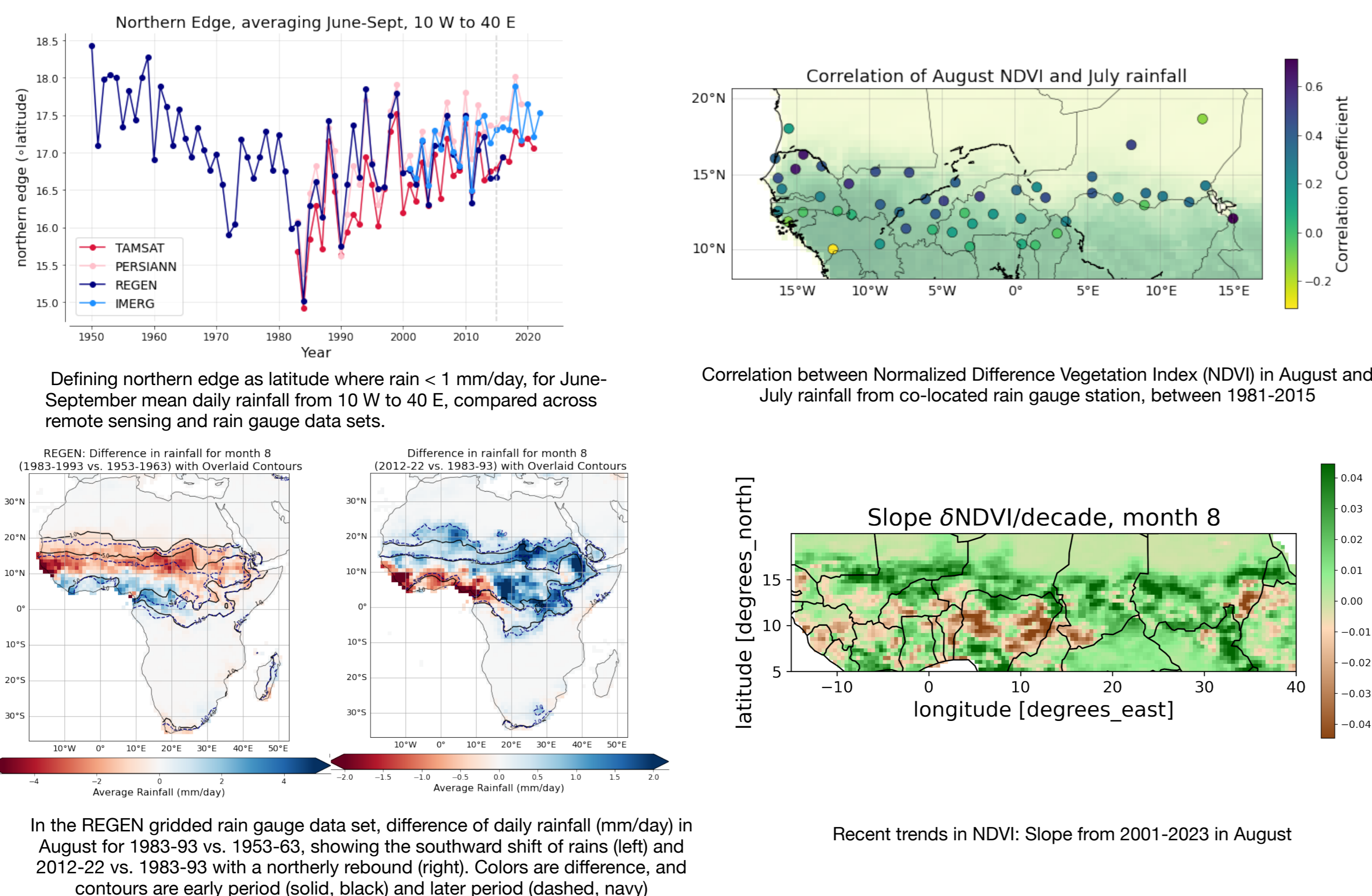


Top, in a simulation in which CO<sub>2</sub> increases at 1%/year and carbon cycle is held constant, June-September mean rain; differences in rainfall from first 10 years of simulation, after 30 years (left) and after 120 years (right panel). Below, an aerosol-only historical simulation.

## Coherent modes of rainfall variability (III)

### North-south shifts in tropical rain belt in Africa

seen in different rain data sets, as well as vegetative greenness (NDVI)



In the REGEN gridded rain gauge data set, difference of daily rainfall (mm/day) in August for 1983-93 vs. 1953-63, showing the southward shift of rains (left) and 2012-22 vs. 1983-93 with a northerly rebound (right). Colors are difference, and contours are early period (solid, black) and later period (dashed, navy)

Recent trends in NDVI: Slope from 2001-2023 in August

## Summary and next steps

- Leading patterns of EOF analysis suggest role for ENSO in first mode of summertime (June-Sept) rainfall, with variability in relative SST warming and land temperature associated with second and third mode
- North-south displacement of rain belt exhibited consistently across rainfall data sets and seen in vegetative greenness trends of Sahel
- These climate models predict less consistent patterns in response to CO<sub>2</sub> than to aerosol forcing
- Next steps include projecting modeled rainfall patterns onto observations & creating 'adaptive' fingerprints that allow for flexibility in the extent and location of predicted patterns; and examining how simulated SST patterns evolve in relation to rainfall, compared to observed SST and rainfall patterns